Dynamic Modelling and Analysis of Three Floating Wind Turbine Concepts with Vertical Axis Rotor

Zhengshun Cheng[1,2], Kai Wang[2,3], Zhen Gao[2,4], Torgeir Moan[2,4]

1 Department of Marine Technology, NTNU, Trondheim, Norway
2 CeSOS, NTNU, Trondheim, Norway
3 NOWITECH, NTNU, Trondheim, Norway
4 AMOS, NTNU, Trondheim, Norway

ABSTRACT

Recently there is an increasing interest in the development of offshore floating vertical axis wind turbines (FVAWTs). A FVAWT mounted on a semi-submersible has been proposed by several researchers, and a FVAWT with a spar buoy has been studied comprehensively in the EU project DeepWind. However, few studies of FVAWT with a TLP floater has been conducted and limited comparative study of FVAWT with different supporting structure has been carried out. In this study, a FVAWT with 5MW Darrieus rotor was used as the reference wind turbine and mounted on three different floating support structures – the OC3 spar buoy, the OC4 semi-submersible and a TLP. Fully coupled nonlinear time domain simulations using the state-of-the-art code Simo-Riflex-DMS were conducted. A series of load cases with turbulent wind and irregular waves were carried out to investigate the dynamic responses of these three FVAWT concepts, such as the generator power production, the platform motions, the tower base bending moments and the mooring line loads. 2P effects are prominent for the three FVAWT concepts. The spar and the semi-submersible can help to mitigate the 2P effects on structural loads and mooring line tensions, at the cost of larger platform motions. The TLP is not a good substructure unless the variation of aerodynamic loads is significantly reduced. The results demonstrate the characteristics of dynamic responses for each FVAWT concept, reveal their advantages and feasibilities and will serve as basis for further developments of the FVAWTs.

KEY WORDS: Floating vertical axis wind turbine; dynamic analysis; spar; semi-submersible; tension leg platform.

INTRODUCTION

As the wind farms are moving towards deeper waters, floating wind turbines will be more economical than the bottom-fixed ones. Floating wind turbines can be categorized as floating horizontal axis wind turbines (FHAWTs) and floating vertical axis wind turbines (FVAWTs). Currently, the FHAWTs are more popular due to their commercial success onshore or near shore. Different platforms for the FHAWTs have been widely studied, including the barge (Vijfhuizen, 2006), spar (Karimirad and Moan, 2012), semi-submersible (Coulling et al., 2013) and TLP (Bachynski and Moan, 2012) types. A number of comparative studies on different FHAWT concepts have been conducted to better understand the performance and to provide basis for further development of each concept. Jonkman and Matha (2011) presented a comprehensive analysis of dynamic responses of three FHAWT concepts based on the NREL 5MW wind turbine mounted on the MIT/NREL TLP, the OC3-Hywind spar buoy and the ITI Energy barge. The concepts are compared based on the ultimate loads, fatigue loads and instabilities. Bachynski et al. (2014) investigated the dynamic responses of a spar, a TLP, and two semi-submersible floating wind turbines in selected misaligned wind and wave conditions with respect to motions and short-term fatigue damage in tower base. The dynamic responses of the four floating wind turbines during pitch actuator fault, grid loss and shut down were studied as well (Bachynski et al., 2013). The motions and structural loads caused by three fault events were compared to the loads encountered in normal operations and extreme conditions.

Efforts on comparative study of HAWTs and VAWTs have been made by several researchers to reveal the merits and feasibilities of each concept, including Paraschivoiu (2002), Islam et al. (2013) and Jamieson (2011). Borg et al. (2014) compared VAWTs with HAWTs in technology, conversion efficiency, upscaling, fatigue, machinery position, etc. Wang et al. (2014) conducted comparative study of a FVAWT with a 5 MW Darrieus rotor and a FHAWT with the NREL 5 MW wind turbine, both mounted on the OC4 semi-submersible platform. As a matter of fact, the FVAWTs have several advantages over the FHAWTs, such as a lower center of gravity, wind direction independence, as well as cost-effective solutions for installation and maintenance, which is attractive for large offshore floating wind turbines. Moreover, the FVAWTs are more suitable for deployment as wind farm when compared to the FHAWTs. For a pair of counter-rotating H-rotors, their wake can dissipate much quicker than those of the FHAWTs, allowing them to be packed closer (Kinzel et al., 2012). Moreover, the average power generated by a pair of H-rotors at all azimuth angles is higher than that of an isolated turbine (Dabiri, 2011), implying that the conversion efficiency of VAWTs can be improved. For these reasons, an increasing interest in the FVAWTs is resurging and various FVAWT concepts are being proposed, including the

DeepWind concept (Paulsen et al., 2011), VertiWind concept (Cahay et al., 2011), etc. Similar to the FHAWTs, the substructures for the FVAWT concepts can also be classified into the spar, semi-submersible and TLP types in terms of how they achieve the static stability. A semi-submersible type FVAWT with a 5MW Darrieus rotor mounted on the OC4 DeepCwind semi-submersible was proposed and analyzed by Wang et al. (2013). A spar type FVAWT with the same rotor placed on the OC3 Hywind spar buoy was also put forward by Borg and Collu (2014) and Cheng et al. (2015). Fully coupled aero-hydro-servo-elastic dynamic simulations were carried out for the FVAWTs. State-of-the-art limited comparative study on different FVAWT concepts have been conducted. Borg and Collu (2014) performed preliminary investigations into the dynamic responses of FVAWTs with the spar, semi and TLP floaters, however the yaw of the spar and the surge and sway of the TLP were disabled during the simulations. Moreover, the structural elasticity and variable speed control were not taken into account.

In order to better understand the performance and benefit of FVAWTs, the current work compares the dynamic response of three FVAWT concepts. A 5MW Darrieus rotor was mounted on three platforms: the OC3 Hywind spar, the OC4 DeepCwind semi-submersible and a TLP design by Bachynski and Moan (2012). The ballast of the spar and the semi, and the tendon pretension of the TLP were adjusted to maintain the same draft and displacement as those supporting the FHAWTs. Fully coupled time domain simulations were carried out using the Simo-Riflex-DMS code, which is an aero-hydro-elastic-servo computational code. A number of load cases were carried out to study the dynamic responses of the three FVAWT concepts. Motions, tower base bending moments and mooring line tensions were calculated and compared. The results reveal the advantages and feasibilities of each FVAWT concept and will help resolve preliminary design trade-offs among the three FVAWT concepts.

FLOATING WIND TURBINE MODELS

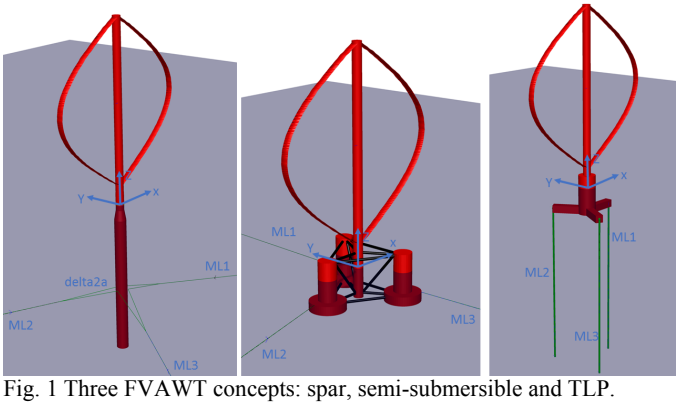

Fig. 1 Three FVAWT concepts: spar, semi-submersible and TLP.

Three floating support structures were studied here: namely a spar, a semi-submersible and a TLP, as depicted in Fig. 1 and listed in Table 2. The concepts were used to support a 5MW Darrieus rotor, which is the baseline design developed in the DeepWind project (Vita, 2011). The rotor is comprised of two blades and one rotating tower that spans from the top to the bottom which is connected to the generator. Main specifications of this rotor are summarized in Table 1. The generator considered here was assumed to be placed at tower base, and the generator mass was incorporated in the platform hull mass.

The concepts were originally designed to support the NREL 5 MW wind turbine (Bachynski et al., 2014). The concepts were considered in the water depth where they were designed, ranging from 150 m for the TLP, 200 m for the semi to 320 m for the spar. Here reasonable modifications were made on each platform to support the 5 MW Darrieus rotor, such as adjusting the ballast of the spar and the semi, and the tendon pretension of the TLP. For each platform, the draft and displacement were maintained the same as the original one. Since the difference in mass between the 5 MW Darrieus rotor and the NREL 5 MW wind turbine was small compared to the displacements of three concepts, it was assumed that such modifications would not alter the hydrostatic performance of each platform significantly, which was verified by the following simulations.

The hydrodynamic model of each concept included a combination of potential flow and Morison's equation. Added mass, radiation damping and first order wave forces were obtained from a potential flow model and applied in the time domain using the convolution technique (Faltinsen, 1995). Second order wave forces were also considered for the spar, the semi and the TLP, respectively. Additional viscous forces on large volume structures were incorporated through Morison's equation. Morison equation was also applied to slender elements which were not included in the potential flow model. Morison coefficients in the hydrodynamic model are those used by Bachynski et al. (2014).

Regarding the structural model of each concept, the platform hull was considered as a rigid body. The tower, blades and shaft were modeled using beam elements; the mooring lines of the spar and the semi were represented using bar elements and the tendon for the TLP was modeled using beam elements and connecting joints.

Spar Structure

The spar platform studied here was the OC3 Hywind hull, as described by Jonkman (2010). The spar consists of two cylindrical regions connected by a linearly tapered conical region. The heavy ballast located at the bottom provides good stability and restoring stiffness, thus limiting the platform pitch and roll motion in wind and waves. A catenary chain mooring system with delta lines and clump weights was applied to approximate the horizontal restoring stiffness as described by Jonkman (2010), schematic layout of the mooring system is illustrated by Karimirad and Moan (2012). Due to the difference in mass between the Darrieus rotor and the NREL 5MW wind turbine, the ballast was adjusted to retain the same draft and displacement specified for the spar FHAWT, leading to changes in the hull mass, center of gravity and moment of inertia, as highlighted in Table 2. The moments of inertia are calculated with respect to the origin of the global coordinate system, as shown in Fig. 1. In addition to the first order and viscous hydrodynamic forces, mean wave drift forces were also applied and Newman's approximation was used to estimate the second-order difference-frequency wave excitation forces.

Semi-submersible Structure

The semi-submersible platform considered here was the OC4 DeepCwind semi-submersible, as defined by Robertson et al. (2012). The semi is composed of three offset columns, three pontoons, a central column and braces. The rotor is located on the central column. Braces are used to connect all of the columns as an integrated body. Three catenary mooring lines are attached to the three offset columns to provide horizontal restoring stiffness. Good stability is achieved by the large waterplane area moment of inertia to limit the pitch and roll motion in wind and waves. The ballast was also adjusted to maintain the same draft and displacement as that of the semi FHAWT described by Robertson et al. (2012). In addition to the first order and viscous forces, the second order difference-frequency wave excitation force

was also considered using full quadratic transfer function (QTF). The effect of second order difference-frequency force on dynamic responses of this semi FVAWT in misaligned wind-wave conditions was studied in Wang et al. (2015c).

Tension Leg Structure

The TLP model considered here was a design by Bachynski and Moan (2012), which is identical as the TLPWT 3. The TLP model consists of one large central column, which approximately contributes to 60% of the displacement, and three pontoons. The stability is obtained by three tendons to limit the global motions in wind and waves. Due to the tendon pretension, the hull mass including ballast and generator is about one half of that corresponding to the displacement, as shown in Table 2. Here the same draft and displacement as the TLP FHAWT were also maintained for the TLP FVAWT, by changing the tendon pretension from 8262 kN to 7450.9 kN. In addition to the first order and viscous hydrodynamic forces, second order difference-frequency wave excitation forces using Newman's approximation and sum-frequency wave excitation forces using full QTF were applied as well.

Table 1. Specifications of the Darrieus 5MW wind turbine

Rated power	5 MW
Rotor height, root-to-root	129.56 m
Rotor radius	63.74 m
Chord length	7.45 m
Airfoil section	NACA0018
Cut-in, rated, cut-out wind speed	5 m/s, 14 m/s, 25 m/s
Rated rotational speed	5.26 rpm
Total mass, including rotor and tower	754226 kg
Center of mass	(0 m, 0 m, 75.6 m)

Table 2. Properties of the three floating platforms

Floater	Spar	Semi	TLP
Water depth [m]	320	200	150
Draft [m]	120	20	22
Waterline diameter [m]	6.5	12.0/6.5	14.0
Hull mass, including ballast and generator [ton]	7308.3	13353.7	2771.9
CM location below MSL [m]	-89.76	-13.42	-15.38
Displacement [m^3]	8027	13919	5655
CB location below MSL [m]	-62.06	-13.15	-14.20
Moment of inertia in roll about global X axis [ton·m^2]	6.362×10^7	9.159×10^6	9.871×10^5
Moment of inertia in pitch about global Y axis [ton·m^2]	6.362×10^7	9.159×10^6	9.871×10^5
Moment of inertia in yaw about platform centerline [ton·m^2]	1.588×10^5	1.209×10^7	2.288×10^5

NUMERICAL SIMULATIONS

Fully Coupled Analysis Tool

Numerical simulations were carried out in order to investigate the dynamic responses of the FVAWTs. The state-of-the-art code Simo-Riflex-DMS, developed by Wang et al. (2013; 2015a), was used to conduct the fully coupled nonlinear time domain simulations. It can account for the turbulent wind inflow, aerodynamics, hydrodynamics, control dynamics, structural mechanics and mooring line dynamics.

Three computer codes are integrated in the code Simo-Riflex-DMS. Simo computes the rigid body hydrodynamic forces and moments on the hull; Riflex represents the blades, tower, shaft and mooring lines as nonlinear bar or beam elements and provides the links to an external controller and DMS; DMS calculates the aerodynamic loads on the rotor according to the Double Multiple-Streamtube (DMS) theory. The generator torque controller was written in Java, which is able to maximize the power capture below the rated operating point and keep the rotational speed constant above the rated operating point. The DMS model accounted for the effect of variation in the Reynolds number and incorporated the Beddoes-Leishman dynamic stall model. The DMS model has been validated by comparison with experimental data (Wang et al., 2015a).

Load Cases and Environmental Conditions

A series of load cases (LCs) were defined to perform the comparative study for the three FVAWT concepts, as summarized in Table 3 and 4. In LC1 free decay tests in surge, heave, pitch and yaw were carried out to assess the natural periods. In LC2, both the unidirectional white noise test and a number of regular wave tests were conducted to estimate the RAOs of the FVAWTs. LC3 are six conditions with correlated and directionally aligned wind and waves.

Table 3. Load case - decay, white noise and regular wave conditions

	Load cases	Response	Wind	Waves
LC1	Decay	Decay	-	Calm water
LC2.1	White noise	RAO	-	White noise
LC2.2	Regular waves	RAO	-	Regular waves

Table 4. Load case - combined wind and wave conditions

LC	U_w [m/s]	H_s [m]	T_p [s]	Turb. Model	Sim. Len. [s]
LC3.1	5	2.10	9.74	NTM	4600
LC3.2	10	2.88	9.98	NTM	4600
LC3.3	14	3.62	10.29	NTM	4600
LC3.4	18	4.44	10.66	NTM	4600
LC3.5	22	5.32	11.06	NTM	4600
LC3.6	25	6.02	11.38	NTM	4600

The three dimensional turbulent wind fields were generated using the NREL's TurbSim program (Jonkman, 2009) according to the Kaimal turbulence model for IEC Class C. Both the normal wind profile (NWP) and normal turbulence model (NTM) was applied. Regarding the NWP condition, the wind profile *U(z)* is the average wind speed as a function of height *z* above the mean sea level (MSL), and is given by the power law as follows

$$U(z) = U_{\text{ref}}(z/z_{\text{ref}})^{\alpha} \quad (1)$$

where U_{ref} is the reference wind speed, z_{ref} the height of reference wind speed and α the power law exponent. The value of z_{ref} was set to 79.78 m (vertical center of the blades) above the MSL. The value of α was chosen to be 0.14 for the floating wind turbines according to IEC

61400-3 (IEC, 2009). The mean wind speed U_w given in Table 4 is the reference wind speed at the vertical center of the blades. The JONSWAP wave model was used to generate the wave history. The significant wave height (H_s) and peak period (T_p) were set in accordance with the correlation with wind speed for the Statfjord site in the northern North Sea (Johannessen et al., 2002).

For the combined wind and wave simulations, each simulation lasted 4600 s and corresponded to a one-hour dynamic analysis, since the first 1000 s was removed to eliminate the start-up transient effects. Five identical and independent one-hour simulations with different seeds for the turbulent wind and irregular waves were carried out for each LC to reduce the stochastic variations. It should be noted here that only LC3.2 and LC3.3 were conducted for the TLP FVAWT, since negative tendon axial forces will arise for large wind speeds. One possible reason for such negative tendon tension is due to the reduction of tendon pretension, but the primary reason is due to the essential characteristics of aerodynamic loads acting on the rotor. The aerodynamic loads are always periodic and are varying with large amplitude, which induce twice-per-revolution (2P) response in platform motions and thus cause large variation of tension in the tendon, as demonstrated in Fig. 6. Fig. 2 also presents the time history of the tendon axial force for the TLP FVAWT in LC3.3. Large variations are observed in the tendon axial forces with period equal to the 2P period. These variations increase with increasing mean wind speed, and give rise to negative axial forces, which is unrealistic.

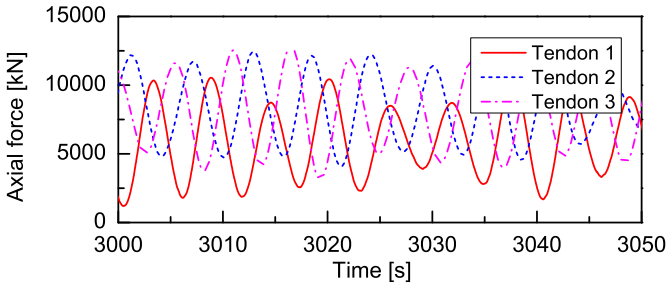

Fig. 2 Time history of the tendon axial forces for the TLP FVAWT in LC3.3 with U_w=14 m/s, H_s=3.62 m, T_p=10.29 s.

RESULTS and DISCUSSIONS

Free Decay Tests

The three floaters considered here are originally designed to support the NREL 5MW baseline wind turbine. When they are used to support the 5MW Darrieus rotor, modifications such as adjusting the ballast for the spar and the semi or reducing the tendon pretension for the TLP have been made to maintain the same draft and displacement as the original ones. Such modifications can lead to changes in the natural periods in the global motions. The natural periods of the three FVAWT concepts are given in Table 5. Free decay tests in the calm water were carried out to estimate the natural periods. In the free decay tests, the wind turbine was parked with rotor plane parallel to the x axis of the global coordinate system as demonstrated in Fig. 1 and no aerodynamic loads acted on the rotor.

In surge and sway, the spar and the semi have very large natural periods due to the relative small surge and sway restoring stiffness of the catenary mooring system employed. In heave, the natural periods of the spar and the TLP are located outside the upper and lower limits of ocean wave periods respectively, while the natural period of the semi is well within the wave excitation range, indicating that significant heave motion for the semi can be excited. In roll and pitch, the natural periods of these three platforms are also well situated outside the wave periods, implying the wave-induced pitch motion will be small. In addition for the TLP FVAWT, due to the rotor orientation, the rotor contributes a lot to the roll/pitch moments of inertia and causes different roll and pitch natural periods. Since the yaw natural period of the spar is well within the wave period, the spar FVAWT may experience significant yaw motion.

Table 5. Natural periods of the three FVAWT concepts obtained by free decay tests.

Floater	Spar	Semi	TLP
Surge/Sway [s]	130.8	114.0	45.3
Heave [s]	27.3	17.1	0.6
Roll/Pitch [s]	34.5	31.0	4.5/4.9
Yaw [s]	8.5	79.7	19.3

Response Amplitude Operators

The hydrodynamic performance of the three floating concepts can be characterized by response amplitude operators (RAOs). The RAOs can be obtained through unidirectional white noise simulations or a number of regular wave simulations. In the present study both white noise simulations and regular wave simulations were performed. The white noise waves were generated using fast Fourier transform (FFT) with a frequency interval $\Delta\omega = 0.005$ rad/s . The surge and pitch RAO are presented in Fig. 3 and 4, respectively. It can be found that the white noise simulation technology captures almost the same natural frequencies as those obtained by the free decay tests. It also predicts all RAOs accurately except at the resonant frequency of each mode. Since the center of gravity of the spar FVAWT is approximately 73.5 m below the MSL, there are close coupling between surge and pitch, resulting in relative large surge RAO at the pitch natural frequency, as illustrated in Fig. 3. As given in Table 5 and demonstrated in Fig. 3 and 4, the natural frequencies of surge and pitch for the spar FVAWT and the semi FVAWT are very close to each other. In addition, the semi FVAWT has much larger RAOs at both surge and pitch resonant frequencies than the spar FVAWT. Regarding the TLP FVAWT, it only exhibits large surge RAOs in the vicinity of the surge natural frequency, and the pitch RAOs are very close to zero as a result of the tensioned tendons.

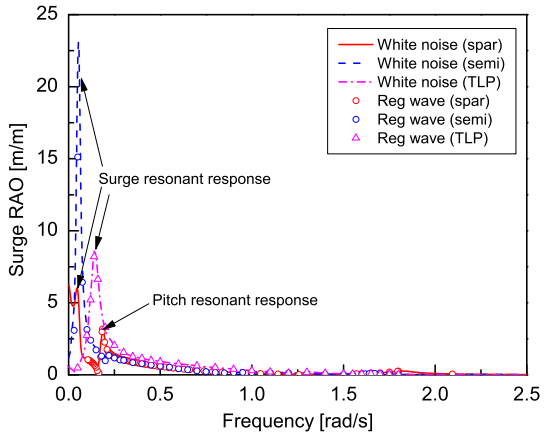

Fig. 3 Surge RAO of the three FVAWT concepts

During the present simulations, the structural elasticity of the curved blades and the tower were taken into account. Peaks corresponding to the elastic blade flatwise mode are thus observed in the pitch RAO for

the spar FVAWT and the semi FVAWT, as presented in Fig. 4. The first 10 eigen modes of the onshore VAWT has been discussed by Wang et al. (2013). It is obvious that the first blade flatwise frequency and the frequencies corresponding to these two peaks for the spar FVAWT and the semi FVAWT do not exactly coincide. These discrepancies comes from the differences in mass and restoring coefficients of the floating platforms, which cause a small shift in the first blade flatwise frequency as compared to the onshore VAWT.

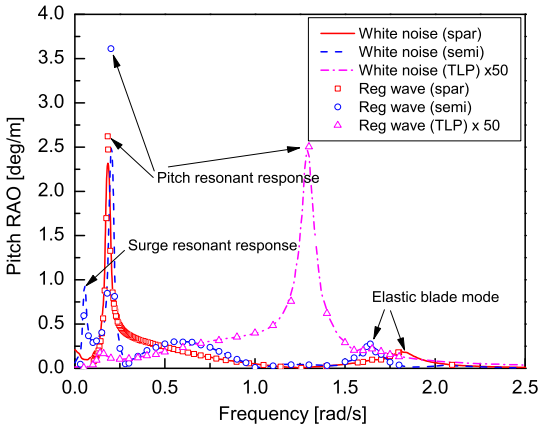

Fig. 4 Pitch RAO of the three FVAWT concepts. The pitch RAO of the TLP FVAWT is multiplied by 50.

Wind Turbine Performance

The stochastic dynamic responses of the three FVAWT concepts are studied under the turbulent wind and irregular wave conditions, including the generator power production, global platform motion, tower base fore-aft and side-to-side bending moment and the tensions of the mooring lines. For each case of each FVAWT model, five identical and independent one-hour simulations were performed; the mean value and standard deviation of the dynamic responses were obtained by averaging the mean values and standard deviations of five 1-h ensembles.

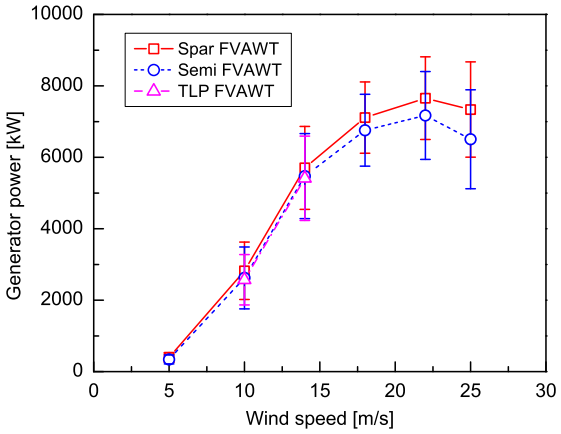

Fig. 5 Mean power production for the three FVAWT concepts with error bar indicating the standard deviation from the mean value.

Fig.5 shows the generator power production of the three FVAWT concepts under the turbulent wind and irregular wave conditions. Hereinafter the results are plotted with the mean wind speed as the variable in the abscissa axis for simplicity. The power curve is based on the mean generator power production with the error bar showing the standard deviation from the mean value. The mean generator powers of the three FVAWT concepts increase as the wind speed increases. At rated wind speed of 14 m/s, the mean generator powers slightly exceed the rated power of 5MW, since the Beddoes-Leishman dynamic stall model is included in the DMS model. The controller implemented is designed to keep the rotational speed constant when the rated operating point is reached, the mean generator powers are therefore keeping increasing at above rated wind speeds. The effects of this non-constant power production at above rated wind speed on the grid can be reduced when the FVAWT are operated as wind farms. Moreover, a more robust controller will be developed in the future to improve the generator power performance for the FVAWT.

In addition, the mean generator powers of the three FVAWT concepts are very close to each other, except at high wind speeds where the mean generator power of the semi FVAWT begins to differ from that of the spar FVAWT. The difference results from the different rotational speed and increases as the wind speed increases. The different rotational speed for the three concepts are due to that the controller implemented in the present is not very robust, it fails to keep the rotational speed at above rated wind speed exactly constant. The variations of the generator power for the three FVAWT concepts are very close to each other as well.

Platform Motion

Due to the differences in structural and hydrodynamic properties and in mooring systems, the three FVAWT concepts present different global motions. The platform motions are defined in the global coordinate system with Z axis along the tower and X axis parallel to the wind direction, as depicted in Fig. 1. Power spectra analysis with frequency smoothing using a parzen window function was used to analyze the time series of global motions. Fig. 6 shows the power spectrum of surge, roll, pitch and yaw motions for the three FVAWT concepts under the turbulent wind and irregular wave conditions with U_w=14 m/s, H_s=3.62 m, T_p=10.29 s, respectively. The responses corresponding to the 2P frequency are observed for each FVAWT. The 2P frequency arises from the characteristic of aerodynamic loads acting on the two-blade vertical axis wind turbine. Since the rotating axis is not parallel to the wind direction, the angle of attack of each blade varies with the azimuth angle of the shaft, leading to the variation of resulting aerodynamic loads within one revolution. For a two-blade FVAWT, the resultant aerodynamic forces and torque varies twice per revolution, and thus gives rise to the 2P frequency responses. The semi FVAWT has larger 2P responses in pitch and roll motions, while the spar FVAWT has large 2P responses in surge and sway motions. These 2P responses increase as the wind speed increases.

Due to the taut mooring system, the spectrum of motions for the TLP FVAWT is much smaller as compared to the spar FVAWT and the semi FVAWT. The surge motions of the three FVAWTs are dominated by the low frequency responses due to the turbulent wind and surge resonant responses. The wave frequency surge responses are larger than the corresponding 2P responses. The spar FVAWT has much larger wind induced surge motion as well as the 2P responses, while the TLP FVAWT has larger wave-frequency surge responses. The spectrum of sway motion differs from the surge spectrum since the wind-induced sway responses of the semi FVAWT is otherwise much larger than that of the spar FVAWT, though the low-frequency wind induced sway responses are both dominating,. For the semi FVAWT, the wind-induced surge and sway is the same order of magnitude, which means the misaligned wind and wave are of interest, which has been studied by Wang et al. (2015b). The heave spectrum of the three FVAWTs is mainly wave-frequency dominated.

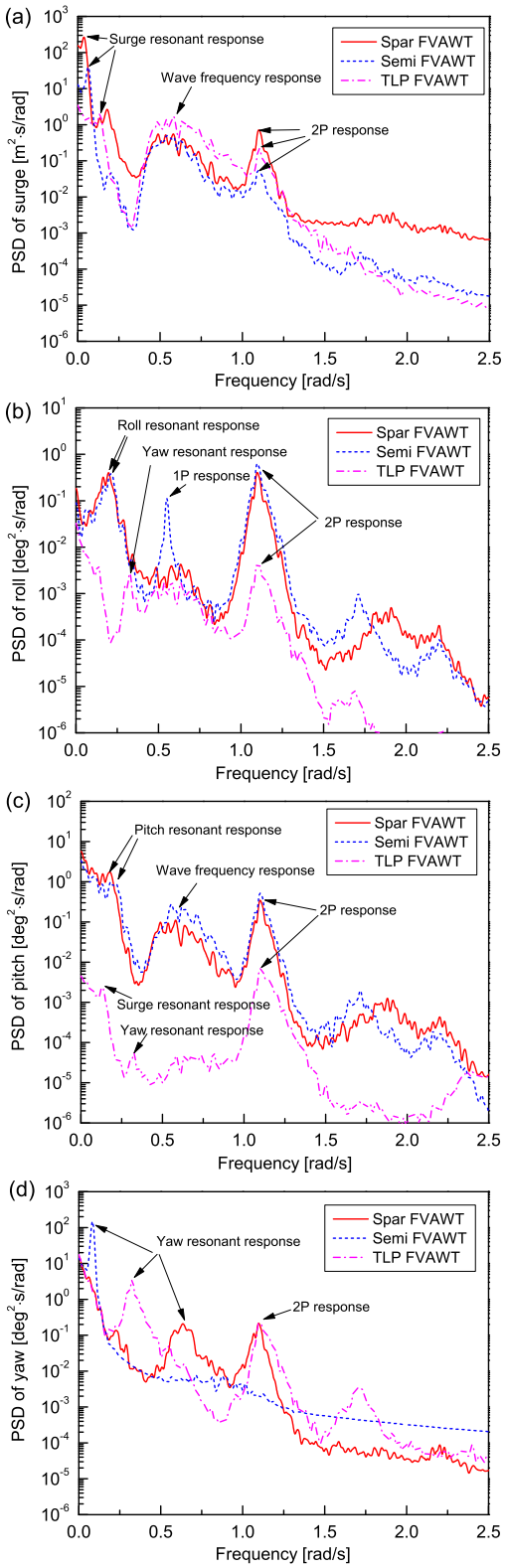

Fig. 6 Power spectra of (a) surge, (b) roll, (c) pitch and (d) yaw motions for the three FVAWT concepts in LC3.3 with U_w=14 m/s, H_s=3.62 m, T_p=10.29 s. Different scales are used in the abscissa axis and ordinate axis.

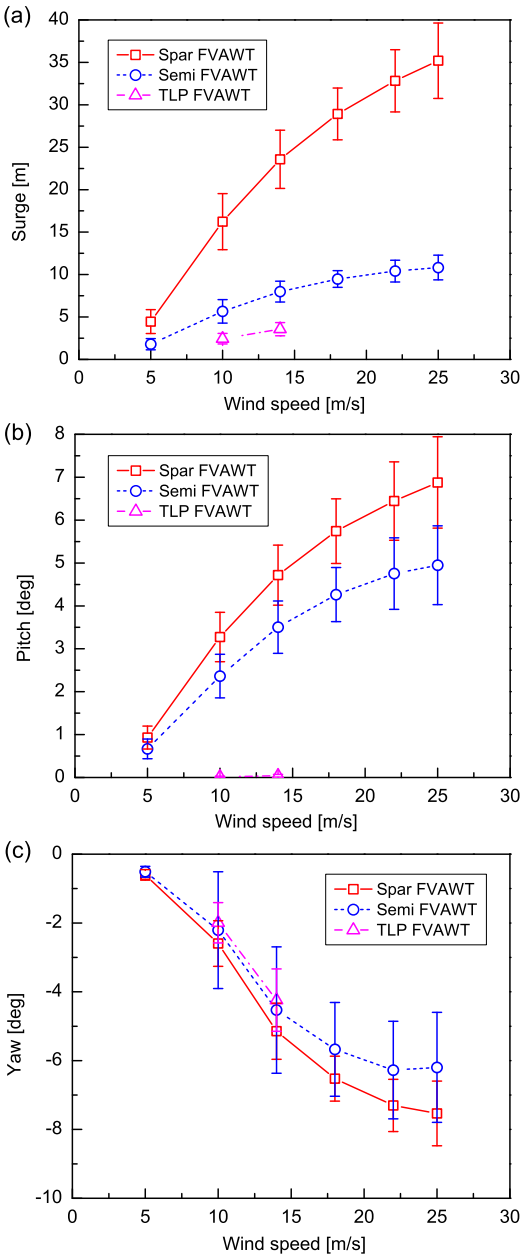

Fig. 7 Mean values of (a) surge, (b) pitch and (c) yaw motions for the three FVAWT concepts with error bar indicating the standard deviation. There are no results for TLP FVAWT at LC 4-6.

The spectrum of pitch motions is very similar to that of the surge motion, as the wind-induced responses and the pitch resonant responses are more dominating. The semi FVAWT has larger wave frequency response and 2P responses in pitch than the spar FVAWT, but the pitch motion of the spar FVAWT is otherwise larger due to the dominating wind-induced responses in the turbulent wind conditions, as shown in Fig. 6(c). The pitch response of the TLP FVAWT is much smaller as compared to the others. Not only the 2P roll response but also the 1P roll response can be observed for the semi FVAWT, as illustrated in Fig. 6(b). The wind induced roll responses are very small, which differs from that of sway responses. Regarding the yaw motion, the yaw responses are also dominated by the turbulent wind induced yaw responses for the three FVAWTs. The yaw motion of the semi FVAWT

is significantly magnified under the turbulent wind condition because the turbulent wind excites the yaw resonant response. For the spar FVAWT and the TLP FVAWT, 2P yaw response is more prominent than the semi FVAWT, this is a consequence of the mooring system used.

Fig. 7 compares the mean values and standard deviations of the global motions of the three FVAWT concepts under the turbulent wind and irregular wave conditions. Here only the results of surge, pitch and yaw motion are presented. The error bar indicates the standard deviation from the mean value. The mean values of the global motion increase as the wind speed increases, since the mean values are mainly wind-induced. For the TLP FVAWT, as a result of the tensioned tendons the vertical motions including the roll, pitch and heave are close to zero, and the surge and sway are also much smaller than those of the spar FVAWT and the semi FVAWT. For the spar FVAWT and the semi FVAWT, the spar FVAWT presents larger mean pitch motion due to the smaller pitch restoring coefficient, but the standard deviations are very close to each other. Since the center of gravity of the spar FVAWT is 73.5 m below MSL, which is much larger than the semi FVAWT, the mean value and standard deviation of surge motion for the spar FVAWT is therefore significantly larger, the mean surge motion reaches 35.20 m under LC3.6. Similar results can be observed for the mean values of roll and sway motions for the spar FVAWT and the semi FVAWT. Though the mean values of each global motion in surge, sway, pitch and roll illustrates significant discrepancies for the three FVAWT concepts, the mean yaw motion are fairly close, as shown in Fig. 7(c). In addition, the standard deviation of yaw of the semi FVAWT is much larger than that of the spar FVAWT, this is due to the resonant yaw motions excited by the turbulent wind.

Tower Base Bending Moment

Here the tower base was assumed to be located below the bearings between the rotating shaft and the drive train shaft. The tower base bending moment is caused by the large aerodynamic force acting on the rotor and by the weight of the rotor due to the tower tilt. Even under the same environmental condition, the three FVAWT concepts demonstrate significant differences in platform motions, leading to discrepancies in the tower base bending moment. Here both the tower base fore-aft bending moment M_{FA} and the side-to-side bending moment M_{SS} are chosen as the primary structural performance parameters. Since the aerodynamic loads of each blade varies with the azimuthal angle, not only M_{FA} but also M_{SS} have great variations, which is quite different from the horizontal axis wind turbine. These variations of bending moments can cause large stress fluctuations, thus leading to great fatigue damage.

Fig. 8 compares the power spectra of M_{FA} and M_{SS} under the turbulent wind and irregular wave condition. The turbulent winds excite the certain low-frequency response of M_{FA}, but the wind-induced response is much smaller than the 2P response in both M_{FA} and M_{SS}. Furthermore, since the taut tendons cannot absorb the 2P aerodynamic excitations for the TLP FVAWT, the 2P responses in M_{FA} and M_{SS} of the spar FVAWT and the semi FVAWT are much smaller than that of the TLP FVAWT, which implies that the catenary mooring system can greatly mitigate the 2P effects on structural dynamic responses. As a consequence, the standard deviations of M_{FA} and M_{SS} for the spar FVAWT and the semi FVAWT are smaller than those of the TLP FVAWT, as shown in Fig. 9. Fig. 9 compares the mean values and standard deviations of M_{FA} for the three FVAWT concepts under different environmental conditions. The mean values and standard deviations of M_{FA} increase as the wind speed increases. The mean values of M_{FA} for the spar FVAWT and the semi FVAWT are much larger than the corresponding standard deviations; on the other hand, the standard deviations of the TLP FVAWT are much larger than the mean values. The spar FVAWT has the largest mean value of M_{FA} with smallest standard deviation. A similar effect is also observed for M_{SS} for the three FVAWT concepts.

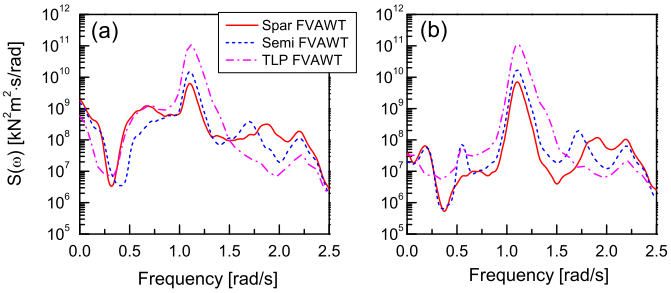

Fig. 8 Power spectra of (a) tower base fore-aft bending moment and (b) tower base side-to-side bending moment for the three FVAWT concepts in LC3.3 with U_w=14 m/s, H_s=3.62 m, T_p=10.29 s.

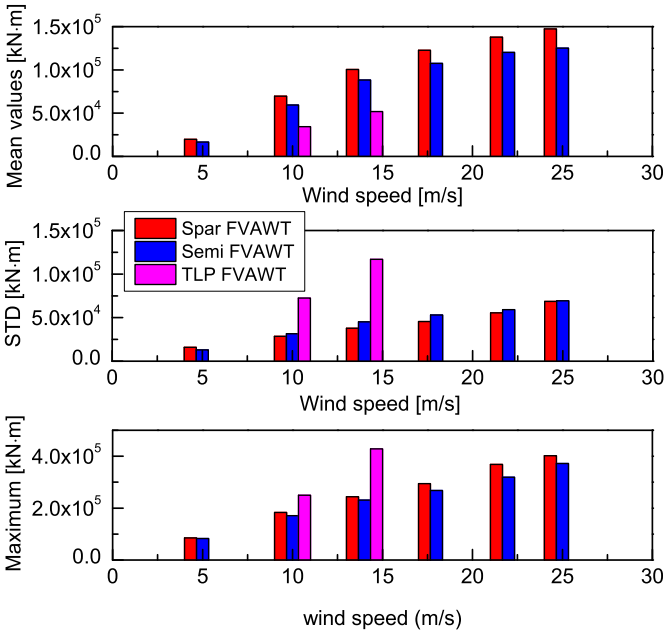

Fig. 9 Mean values, standard deviations and maximum values of the tower base fore-aft bending moment for the three FVAWT concepts. There are no results for TLP FVAWT at LC 4-6.

Mooring Line Tension

The mooring system is used to keep the platform in position. Due to the large aerodynamic excitations at high wind speeds, the FVAWT may experience large global motion, especially the yaw motion as shown in Fig. 7(c). The three FVAWT concepts used different mooring systems, as depicted in Fig. 1. The TLP FVAWT employed the three pretension tendons, which results in large 2P variation of tension in the tendons, as demonstrated in Fig. 2. The TLP is a desirable supporting structure choice when the variations of the aerodynamic loads acting on the rotor are reduced significantly. Actually this can be achieved by increasing the blade number or using helical blade (Cahay et al., 2011). One chain mooring system with delta lines and clump weights was applied for the spar FVAWT, and one catenary mooring system was adopted by the semi FVAWT. In the present study, the mooring line tensions at the fairlead were studied, Fig. 10 presents the power spectrum of the

tension of mooring line 2 for the semi and TLP FVAWTs and delta line 2a for the spar FVAWT under turbulent wind and irregular wave condition. The mooring lines in the global coordinate system is specified in Fig. 1 for three FVAWT concepts, respectively.

The power spectral density of the tension for the TLP FVAWT is approximately three order of magnitude higher than that of the semi FVAWT and the spar FVAWT, since the variations of tendon tensions are too large as compared to the other two. For the spar and semi FVAWTs, the turbulent wind induced response of the tension of mooring line is dominating, and the contributions from the wave frequency response and 2P response increase as the significant wave height and wind speed increase. Additionally for the spar FVAWT the delta line tensions are always remaining positive, meaning that the current mooring system is acceptable for the operational condition. Moreover, the mean value, standard deviation and maximum values of the semi FVAWT are all larger than that of the spar FVAWT, as shown in Fig. 11.

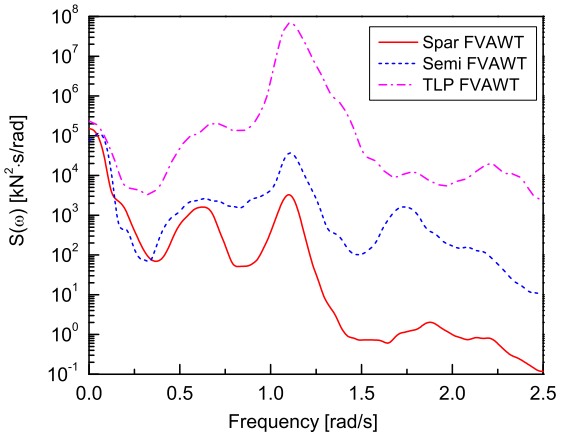

Fig. 10 Power spectrum of the tension in delta line 2a for the spar FVAWT and mooring line 2 for the semi and TLP FVAWTs in LC3.3 with U_w=14 m/s, H_s=3.62 m, T_p=10.29 s.

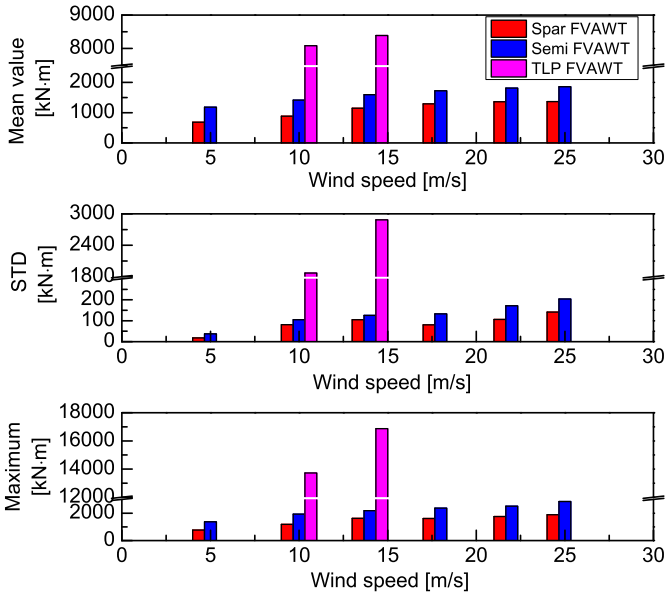

Fig. 11 Mean values, standard deviations and maximum values of the tension in delta line 2a for the spar FVAWT and mooring line 2 for the semi and TLP FVAWTs. There are no results for TLP FVAWT at LC 4-6.

CONCLUSIONS

The present paper deals with a comparative study of the dynamic responses of three floating vertical axis wind turbine concepts. The OC3 spar, the OC4 semi-submersible and a TLP, which were originally designed to support the NREL 5MW wind turbine, were taken as the floating platform to support a 5MW Darrieus rotor. The ballast of the spar and the semi and the tendon pretension of the TLP were adjusted to maintain the same draft and displacement as those supporting the FHAWTs. Fully coupled time domain simulations were carried using the Simo-Riflex-DMS code. The natural periods and RAOs of the floating systems were firstly estimated to identify the hydrodynamic properties through free decay tests, white noise test and regular wave test, respectively. A series of load cases with turbulent wind and irregular waves were then defined to investigate global stochastic dynamic responses of the three FVAWT concepts, including the generator power production, the platform motions, the tower base bending moment and the tensions of mooring lines.

Both the mean values and the standard deviations of the generator power production for the three FVAWTs are very close, except that differences in mean power between the spar FVAWT and the semi FVAWT arise due to the different rotor rotational speeds. For the three FVAWTs, the motion of surge, pitch and yaw are mainly due to the low-frequency turbulent wind loads, and the responses corresponding to the 2P frequency are observed for each motion. The spar FVAWT suffers the largest mean value and standard deviation of motions in surge, pitch and yaw. The semi FVAWT displays the best global motion performance. Though the three FVAWTs experience severe yaw motion especially at high wind speed, the yaw motion of the semi FVAWT is mainly caused by the wind induced yaw resonant response, attention should be paid to the yaw natural period when designing a semi-submersible for FVAWT.

Significant 2P effects can be observed in the responses of the tower base bending moments for the three FVAWTs. These 2P responses can cause great fatigue damage and should be reduced, e.g. by damping. The slack mooring lines can mitigate the 2P effects since they are more efficient to absorb the 2P aerodynamic excitations. In addition, the 2P variations in the aerodynamic loads can be relieved by introducing more blades or helical blades despite the increasing costs. Large variations of axial force also exist in the tendons of the TLP FVAWT due to the 2P aerodynamic loads. Unless these variations are significantly reduced, the TLP is not a very good supporting structure. The present mooring system with clump weight and delta lines for the spar FVAWT can only work well for the operational condition, a new mooring system is required when the extreme condition analysis is carried out. Both the mooring line tensions for the semi FVAWT and the delta line tensions for the spar FVAWT show obvious 2P response, but they are much smaller than those for the TLP FVAWT.

Although the three floating platforms are originally designed to support the NREL 5 MW wind turbine, the present study aims to reveal the dynamic response characteristics of each FVAWT concept. The results can help resolve preliminary design trade-offs among the three FVAWT concepts and will serve as basis for further developments of each FVAWT concept.

ACKNOWLEDGEMENTS

The authors would like to acknowledge the financial support from the EU FP7 project MARE WINT (project no 309395) through the Centre for Ships and Ocean Structures at the Department of Marine Technology, Norwegian University of Science and Technology,

Trondheim, Norway. The first author would also like to thank Dr. Erin Bachynski from MARINTEK for providing the TLP model and kindly help on using the simulation codes.

REFERENCES

Bachynski, EE, and Moan, T (2012). "Design considerations for tension leg platform wind turbines," *Marine Structures*, *29*(1), 89-114.

Bachynski, EE, Kvittem, MI, Luan, C, and Moan, T (2014). "Wind-Wave Misalignment Effects on Floating Wind Turbines: Motions and Tower Load Effects," *Journal of Offshore Mechanics and Arctic Engineering*, *136*(4), 041902.

Bachynski, EE, Etemaddar, M, Kvittem, MI, Luan, C, and Moan, T (2013). "Dynamic Analysis of Floating Wind Turbines During Pitch Actuator Fault, Grid Loss, and Shutdown," *Energy Procedia*, *35*, 210-222.

Borg, M, and Collu, M (2014). "A Comparison on the Dynamics of a Floating Vertical Axis Wind Turbine on Three Different Floating Support Structures," *Energy Procedia*, *53*, 268-279.

Borg, M, Shires, A, and Collu, M (2014). "Offshore floating vertical axis wind turbines, dynamics modelling state of the art. part I: Aerodynamics," *Renewable and Sustainable Energy Reviews*.

Cahay, M, Luquiau, E, Smadja, C, and Silvert, F (2011). "Use of a vertical wind turbine in an offshore floating wind farm," *Offshore Technology Conference*, Houston, Texas, USA.

Cheng, Z, Wang, K, Gao, Z, and Moan, T (2015). "Comparative study of spar type floating horizontal and vertical axis wind turbines subjected to constant winds," *Proceedings of EWEA Offshore 2015*, Copenhagen, Denmark.

Coulling, AJ, Goupee, AJ, Robertson, AN, Jonkman, JM, and Dagher, HJ (2013). "Validation of a FAST semi-submersible floating wind turbine numerical model with DeepCwind test data," *Journal of Renewable and Sustainable Energy*, *5*(2), 023116.

Dabiri, JO (2011). "Potential order-of-magnitude enhancement of wind farm power density via counter-rotating vertical-axis wind turbine arrays," *Journal of Renewable and Sustainable Energy*, *3*(4), 043104.

Faltinsen, OM (1995). Sea loads on ships and offshore structures, Cambridge University Press, Cambridge, UK.

IEC (2009). "International Standard 61400-3, Wind turbines, Part 3: Design requirements for offshore wind turbines.

Islam, MR, S.Mekhilef, and R.Saidur (2013). "Progress and recent trends of wind energy technology," *Renewable and Sustainable Energy Reviews*, *21*, 456-468.

Jamieson, P (2011). Innovation in wind turbine design, John Wiley & Sons.

Johannessen, K, Meling, TS, and Haver, S (2002). "Joint distribution for wind and waves in the northern north sea," *International Journal of Offshore and Polar Engineering*, *12*(1).

Jonkman, BJ (2009). TurbSim user's guide: Version 1.50. , Tech. Rep. NREL/TP-500-46198, NREL, Golden, CO, USA.

Jonkman, J (2010). Definition of the floating system for Phase IV of OC3, Tech. Rep. NREL/TP-500-47535, NREL, Golden, CO, USA.

Jonkman, JM, and Matha, D (2011). "Dynamics of offshore floating wind turbines-analysis of three concepts," *Wind Energy*, *14*(4), 557-569.

Karimirad, M, and Moan, T (2012). "Wave and wind induced dynamic response of a spar-type offshore wind turbine," *Journal of Waterway, Port, Coastal, and Ocean Engineering*, *138*(1), 9–20.

Kinzel, M, Mulligan, Q, and Dabiri, JO (2012). "Energy exchange in an array of vertical-axis wind turbines," *Journal of Turbulence*, *13*(38), 1-13.

Paraschivoiu, I (2002). Wind turbine design: with emphasis on Darrieus concept, Polytechnic International Press. , Montreal, Canada.

Paulsen, US, Pedersen, TF, Madsen, HA, Enevoldsen, K, Nielsen, PH, Hattel, JH, Zanne, L, Battisti, L, Brighenti, A, and Lacaze, M (2011). "Deepwind-an innovative wind turbine concept for offshore," *European Wind Energy Association (EWEA) Annual Event*, Brussels.

Robertson, A, Jonkman, J, Masciola, M, Song, H, Goupee, A, Coulling, A, and Luan, C (2012). Definition of the Semisubmersible Floating System for Phase II of OC4, NREL, Golden, CO, USA.

Vijfhuizen, W (2006). Design of a Wind and Wave Power Barge, Universities of Glasgow and Strathclyde, Glasgow, Scotland.

Vita, L (2011). Offshore Floating Vertical Axis Wind Turbines with Rotating Platform, Technical University of Denmark, Roskilde, Denmark.

Wang, K, Moan, T, and Hansen, MOL (2013). "A method for modeling of floating vertical axis wind turbine," *Proceedings of the 32th International Conference on Ocean, Offshore and Arctic Engineering*, OMAE2013-10289, Nantes, France.

Wang, K, Hansen, MOL, and Moan, T (2015a). "Model improvements for evaluating the effect of tower tilting on the aerodynamics of a vertical axis wind turbine," *Wind Energy*, *18*, 91-110.

Wang, K, Moan, T, and Hansen, MOL (2015b). "Stochastic dynamic response analysis of a floating vertical axis wind turbine with a semi-submersible floater," *Wind Energy*, *(submitted)*.

Wang, K, Luan, C, Moan, T, and Hansen, MOL (2014). "Comparative Study of a FVAWT and a FHAWT with a Semi-submersible Floater," *Proceedings of the 24th International Ocean and Polar Engineering Conference*, Busan, Korea.

Wang, K, Cheng, Z, Moan, T, and Hansen, MOL (2015c). "Effect of difference-frequency forces on the dynamics of a semi-submersible type FVAWT in misaligned wave-wind condition," *Proceedings of the 25th International Ocean and Polar Engineering Conference*, Kona, Big Island, Hawaii, USA.